CAPON AND APES SPECTRUM ESTIMATION FOR REAL-VALUED SIGNALS

Andreas Jakobsson[1]

Systems and Control Group
Box 27, SE-751 03 Uppsala
Sweden.

Torbjörn Ekman[2]

Signals and Systems Group
Box 528, SE-751 20 Uppsala
Sweden.

Petre Stoica

Systems and Control Group
Box 27, SE-751 03 Uppsala
Sweden.

ABSTRACT

This paper considers the problem of estimating the spectrum of real-valued signals. We propose real-valued versions of the Capon and the APES spectral estimators. The estimators are derived as members of the Matched-Filterbank (MAFI) estimator class as introduced in [1]. Furthermore, we show that the real-valued estimators will be unbiased, whereas the complex-valued estimators will have a (slight) bias for real-valued data. Finally, we conclude the paper with a numerical example illustrating the performance of the proposed estimators.

1. INTRODUCTION

In the filterbank approach to spectral estimation, the amplitude of the spectrum is estimated by passing the signal through a narrowband filter, $\mathbf{h}_\omega$, with varying center frequency ω (see, e.g., [2]). Here, and in the following, the subscript ω is used to indicate a parameter's dependence on the filter's center frequency. Let $\{y(t); t = 1, \ldots, N\}$ denote the available (stationary) data sample of which the spectrum is to be estimated, where N denotes the number of data samples. The filter output can then be written as:

$$\mathbf{h}_\omega^* \mathbf{y}(t) \approx \alpha(\omega) e^{i\omega t} + e(t), \tag{1}$$

for $t = 1, \ldots, M$, where $M = N - L + 1$,

$$\mathbf{y}(t) = \left[\begin{array}{ccc} y(t) & \ldots & y(t+L-1) \end{array} \right]^T, \tag{2}$$

$(\cdot)^T$ and $(\cdot)^*$ denote transpose and complex conjugate transpose, respectively, and $e(t)$ is some additive colored noise.

This work was supported in part by the Swedish Institute, the Senior Individual Grant Programme of the Swedish Foundation for Strategic Research and the Royal Swedish Academy of Sciences.

[1]Andreas Jakobsson is currently on leave at Dept. of Elec. & Comp. Eng., Brigham Young University, Provo, UT 84602, USA.

[2]Torbjörn Ekman is currently on leave at Institut für Nachrichtentechnik und Hochfrequenztechnik, Technische Universität Wien, Gusshausstrasse 25 / 389, A- 1040 Wien, Austria.

The least-squares estimate of the complex amplitude, $\alpha(\omega)$, in (1) is then given by

$$\hat{\alpha}(\omega) = \mathbf{h}_\omega^* \mathbf{Y}_\omega \tag{3}$$

where

$$\mathbf{Y}_\omega = \frac{1}{M} \sum_{t=1}^{M} \mathbf{y}(t) e^{-i\omega t}. \tag{4}$$

The problem of designing $\mathbf{h}_\omega$ as a matched-filterbank (MAFI) was studied in [1]. It was found that the well-known Capon method [3, 4], as well as the recently proposed APES (Amplitude and Phase Estimation of a Sinusoid) method [2], can be interpreted as members of the MAFI class. The corresponding filters are designed as:

$$\mathbf{h}_\omega^{Capon} = \hat{\mathbf{R}}^{-1} \mathbf{a}_\omega \left(\mathbf{a}_\omega^* \hat{\mathbf{R}}^{-1} \mathbf{a}_\omega \right)^{-1} \tag{5}$$

$$\mathbf{h}_\omega^{APES} = \hat{\mathbf{Q}}_\omega^{c-1} \mathbf{a}_\omega \left(\mathbf{a}_\omega^* \hat{\mathbf{Q}}_\omega^{c-1} \mathbf{a}_\omega \right)^{-1} \tag{6}$$

where the estimate of the (complex-valued data) noise covariance matrix, $\hat{\mathbf{Q}}_\omega^c$, is found as (see [1])

$$\hat{\mathbf{Q}}_\omega^c = \hat{\mathbf{R}} - \mathbf{Y}_\omega \mathbf{Y}_\omega^*, \tag{7}$$

and

$$\hat{\mathbf{R}} = \frac{1}{M} \sum_{1}^{M} \mathbf{y}(t) \mathbf{y}(t)^* \tag{8}$$

$$\mathbf{a}_\omega = \left[\begin{array}{cccc} 1 & e^{i\omega} & \ldots & e^{i(L-1)\omega} \end{array} \right]^T. \tag{9}$$

Many signals are actually *real-valued* which the above filter design does not exploit. For such signals, it is more appropriate to design the filter taking into account the fact that the spectrum is *symmetric*.

In the following section we present a real-valued version of the Capon and APES spectral estimators. In section 3, we then discuss these estimators bias in the case of real-valued data. Finally, we conclude in section 4 with a numerical simulation illustrating the proposed estimators performance.

2. THE REAL-VALUED MAFI APPROACH

It is reasonable to expect better performance of the real-valued filter design because by construction the filters will pass both frequencies of interest, ω and $-\omega$, undistorted, whereas the complex-valued design above will only pass ω undistorted, and will try to null $-\omega$, therefore yielding less power in the filtered output.

The filterbank approach basically reduces the problem of estimating the spectrum of $y(t)$ to that of estimating the amplitude of a sinusoidal signal buried in colored noise (see, e.g., [2, 5]). Therefore, under the assumption of real-valued data, it is reasonable to consider $y(t)$ to be additively decomposed as:

$$y(t) = r_\omega \sin(\omega t + \varphi_\omega) + n(t) \tag{10}$$

where $r_\omega \in \mathbb{R}$, $\omega \in (0, 2\pi]$ and $n(t)$ is some additive colored noise. By rewriting (10) as:

$$y(t) = a_\omega \cos(\omega t) + b_\omega \sin(\omega t) + n(t), \tag{11}$$

where

$$\begin{aligned} \varphi_\omega &= \arctan\left(\frac{a_\omega}{b_\omega}\right) && (12)\\ r_\omega &= \sqrt{a_\omega^2 + b_\omega^2}, && (13) \end{aligned}$$

we can write $\mathbf{y}(t)$ as:

$$\mathbf{y}(t) = \mathbf{A}_\omega \mathbf{u}(t) + \mathbf{n}(t), \tag{14}$$

where $\mathbf{n}(t)$ is formed in the same way as $\mathbf{y}(t)$, and

$$\begin{aligned} \mathbf{A}_\omega &= \begin{bmatrix} 1 & 0 \\ \cos\omega & \sin\omega \\ \vdots & \vdots \\ \cos(L-1)\omega & \sin(L-1)\omega \end{bmatrix} && (15)\\ \mathbf{u}(t) &= \begin{bmatrix} \cos(\omega t) & \sin(\omega t) \\ -\sin(\omega t) & \cos(\omega t) \end{bmatrix} \theta_\omega && (16)\\ &= \Theta_\omega \mathbf{v}_t^T, && (17) \end{aligned}$$

where

$$\begin{aligned} \theta_\omega &= \begin{bmatrix} a_\omega & b_\omega \end{bmatrix}^T && (18)\\ \Theta_\omega &= \begin{bmatrix} a_\omega & b_\omega \\ b_\omega & -a_\omega \end{bmatrix} && (19)\\ \mathbf{v}_t &= \begin{bmatrix} \cos(\omega t) & \sin(\omega t) \end{bmatrix}. && (20) \end{aligned}$$

As in the complex-valued case (see [1]), the choice of the filterlength, L, should be done by a compromise between resolution and statistical stability: the larger L the better the resolution but the worse the statistical stability.

Following the MAFI design in [1], the real-valued MAFI filter is designed such that the corresponding signal-to-noise ratio (SNR) in the filter's output is maximized:

$$\max_{\mathbf{h}_\omega} \frac{\|\mathbf{h}_\omega^T \mathbf{A}_\omega\|^2}{\mathbf{h}_\omega^T \hat{\mathbf{Q}}_\omega^r \mathbf{h}_\omega} \tag{21}$$

where $\|\cdot\|$ denotes the vector norm, the filter is constrained as (c.f., (14) and (16))

$$\mathbf{h}_\omega^T \mathbf{A}_\omega = \begin{bmatrix} 1 & 0 \end{bmatrix} \triangleq \mathbf{c}^T, \tag{22}$$

and $\hat{\mathbf{Q}}_\omega^r$ is an estimate of the (real-valued data) noise covariance matrix. The maximization in (21), under the constraint (22), can easily be found to be equivalent to

$$\min_{\mathbf{h}_\omega} \mathbf{h}_\omega^T \hat{\mathbf{Q}}_\omega^r \mathbf{h}_\omega \quad \text{subject to} \quad \mathbf{h}_\omega^T \mathbf{A}_\omega = \mathbf{c}^T, \tag{23}$$

which is a well-known, well-studied, minimization problem (see, e.g., [6]). The real-valued version of the Capon and APES estimators (termed rv-Capon and rv-APES) can then be found as (c.f., (5) and (6))

$$\begin{aligned} \mathbf{h}_\omega^{rv-Capon} &= \hat{\mathbf{R}}^{-1}\mathbf{A}_\omega \left(\mathbf{A}_\omega^T \hat{\mathbf{R}}^{-1} \mathbf{A}_\omega\right)^{-1} \mathbf{c} && (24)\\ \mathbf{h}_\omega^{rv-APES} &= \hat{\mathbf{Q}}_\omega^{r-1}\mathbf{A}_\omega \left(\mathbf{A}_\omega^T \hat{\mathbf{Q}}_\omega^{r-1} \mathbf{A}_\omega\right)^{-1} \mathbf{c}. && (25) \end{aligned}$$

Using (17), the estimate of the data covariance matrix can be written as:

$$\hat{\mathbf{R}} = (\widehat{\mathbf{A}_\omega \Theta_\omega}) \mathbf{G} (\widehat{\mathbf{A}_\omega \Theta_\omega})^T + \hat{\mathbf{Q}}_\omega^r \tag{26}$$

where

$$\mathbf{G} = \frac{1}{M} \sum_{t=1}^{M} \mathbf{v}_t^T \mathbf{v}_t. \tag{27}$$

From (14), the least squares estimate of $\mathbf{A}_\omega \Theta_\omega$, ignoring the fact that $\mathbf{A}_\omega$ is known, is given by:

$$(\widehat{\mathbf{A}_\omega \Theta_\omega}) = \hat{\mathbf{C}}_\omega \mathbf{G}^{-1} \tag{28}$$

where

$$\hat{\mathbf{C}}_\omega = \frac{1}{M} \sum_{t=1}^{M} \mathbf{y}(t) \mathbf{v}_t. \tag{29}$$

Finally, inserting (28) into (26) yields the following estimate of $\hat{\mathbf{Q}}_\omega^r$ (c.f. (7))

$$\hat{\mathbf{Q}}_\omega^r = \hat{\mathbf{R}} - \hat{\mathbf{C}}_\omega \mathbf{G}^{-1} \hat{\mathbf{C}}_\omega^T. \tag{30}$$

By using equation (22) and the structure in (16), a least-squares estimator of θ_ω can then be formulated as:

$$\hat{\theta}_\omega = \mathbf{G}^{-1} \hat{\mathbf{C}}_\omega^T \mathbf{h}_\omega \tag{31}$$

where $\mathbf{h}_\omega$ denotes either the Capon or the APES-filter in (24) and (25), respectively. Then take $\hat{r}_\omega$, using (13) and the estimates in (31), as an estimate of the spectrum of $y(t)$ at frequency ω.

From a computational viewpoint, it is here worth mentioning that the calculation of $\hat{\mathbf{Q}}_\omega^{r\,-1}$ in (25) can be done efficiently by expanding the inversion of $\hat{\mathbf{Q}}_\omega^r$ using the matrix inversion lemma (see, e.g., [6]). Furthermore, note that $\mathbf{G}^{-1}$ in (30) can be calculated in a closed form expression and that the sum in (29) can be efficiently computed using the real and imaginary part of the FFT.

Also, note that in the cases where $\sin(\omega t) \approx 0$ (and similarly for $\cos(\omega t)$) the inversions needed to calculate (24), (25) and (31) will need special solutions (which are easily derived) due to the fact that the matrices will be singular.

3. BIAS ANALYSIS

To examine the behavior of the complex-valued Capon and APES spectral estimators on real-valued data, we reformulate the data model in (10) using Euler's formulas. The sample vector $\mathbf{y}(t)$ in (2) can then be expressed as:

$$\mathbf{y}(t) = \alpha_\omega \mathbf{a}_\omega e^{i\omega t} + \alpha_\omega^* \mathbf{a}_{-\omega} e^{-i\omega t} + \mathbf{n}(t), \qquad (32)$$

where $\alpha_\omega = (r_\omega/2)e^{i(\varphi_\omega - \pi/2)}$. The least squares estimator in (3) can then be written as:

$$\hat{\alpha}_\omega = \alpha_\omega + \alpha_\omega^* L M^{-1} e^{i\omega} \overline{H_\omega(-\omega)\rho(M,\omega)} + h_\omega^* \Delta_\omega, \quad (33)$$

where $\overline{(\cdot)}$ denotes complex conjugate, the frequency response of the filter h_ω at frequency f, $H_\omega(f)$, is found as:

$$H_\omega(f) = \frac{1}{L}\sum_{k=1}^{L} h_\omega(k) e^{-ifk} = L^{-1} e^{-if} h_\omega^T \overline{\mathbf{a}}_f, \qquad (34)$$

and, where

$$\rho(M,\omega) = \sum_{t=1}^{M} e^{i2\omega t} \qquad (35)$$

$$= e^{i(M+1)\omega} \frac{\sin(M\omega)}{\sin(\omega)} \qquad (36)$$

$$\Delta_\omega = \frac{1}{M}\sum_{t=1}^{M} n(t) e^{-i\omega t}. \qquad (37)$$

Following the discussion in [1], the expected value for the estimation error in (33) can be expressed as:

$$E(\hat{\alpha}_\omega - \alpha_\omega) = \alpha_\omega^* L M^{-1} e^{i\omega} \overline{H_\omega(-\omega)\rho(M,\omega)}, \qquad (38)$$

where $E(\cdot)$ denotes expectation. Since $\rho(M,\omega)$ in (38) is an oscillating function, and as $H_\omega(-\omega)$, although small, will be non-zero, the complex-valued estimators *will have* a (slight) bias (at most frequencies) for real-valued data. It should be noted that, even though the methods are biased on real-valued signals, this bias will in most cases be small. The methods will treat the contribution from $\alpha_\omega^* e^{-i\omega t}$ as part of the noise and will thus try to minimize it's influence.

A similar procedure for the least-squares estimate for the real-valued spectral estimators will indicate that they are unbiased. The estimation error in (31) can, by inserting the expression for $\hat{\mathbf{C}}_\omega$ in (29), be rewritten as in (39), at the top of the next page. The estimate of the spectrum, $\hat{r}_\omega$, as given by (13), will thus be unbiased.

4. NUMERICAL EXAMPLE

As the finite-sample performance analysis of the spectral estimators is quite difficult at best, we illustrate the performance using numerical simulations. In this section we study how the estimators performance depends on the signal-to-noise ratio (SNR). Figure 1 shows the modulus of the true spectrum which consists of three superimposed real-valued sinusoids located at the following frequencies: $0.1475, 0.1850, 0.2194$ (where 1 is the sampling frequency). The sinusoids have initial phases $0.2\pi, 0.6\pi, 0.2\pi$. The data sequence has $N = 64$ data samples and is corrupted by a zero mean white Gaussian noise with standard deviation σ. The SNR for the kth sinusoid is defined as

$$\text{SNR}_k = 10\log\frac{r_k^2}{\sigma^2} \quad [\text{dB}] \qquad (40)$$

where r_k is the amplitude of the kth sinusoid. In the simulated data these were $0.3, 2, 1$.

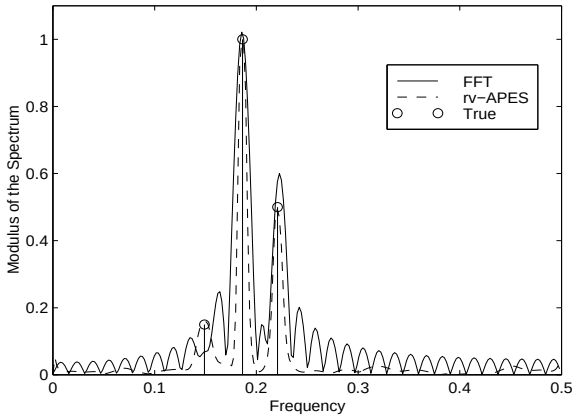

Figure 1: The modulus of the true spectrum, plotted together with the periodogram and the rv-APES spectral estimate, SNR=25dB.

The filterlength, L, was set to 20 taps. To obtain a reasonably fine grid on the frequency axis the spectrum was evaluated at 256 grid points. In Figure 1 the limited amount

$$E\left(\hat{\theta}_\omega - \theta_\omega\right) = E\left(\mathbf{G}^{-1}\frac{1}{M}\sum_{t=1}^{M}\mathbf{v}_t^T\mathbf{v}_t\theta_\omega\right) + E\left(\mathbf{G}^{-1}\frac{1}{M}\sum_{t=1}^{M}\mathbf{v}_t^T h_\omega^T\mathbf{n}(t)\right) - \theta_\omega = \theta_\omega + 0 - \theta_\omega = 0 \qquad (39)$$

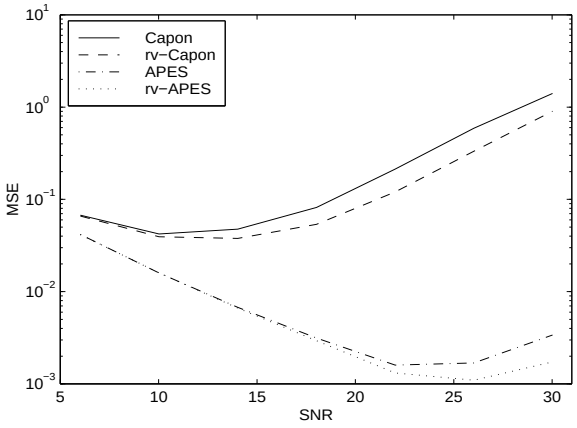

Figure 2: The presented estimators' MSE as the SNR varies.

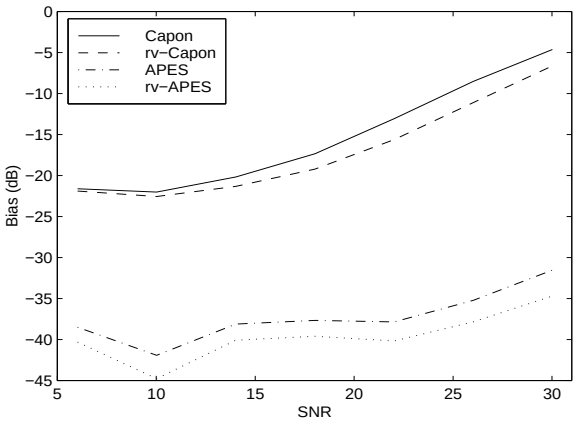

Figure 3: The presented estimators' bias as the SNR varies.

of data gives a corrupted periodogram, while the rv-APES manage to reproduce the true spectrum quite accurately.

Figure 2 shows the mean square error (MSE) of the Capon (solid line), rv-Capon (dashed line), APES (dash-dotted line) and rv-APES (dotted-line) spectral estimators for the second frequency as the SNR varies. As can be seen, the proposed estimators perform better than their complex counterparts. Note that the reason why the MSE increases for high SNR is that $\hat{\mathbf{R}}$ becomes almost singular.

Figures 3 and 4 shows the estimators bias and variance, respectively, and as was expected the real-valued estimators have a somewhat lower bias than their complex-valued counterparts. It can also be seen, in Figure 4, that the rv-

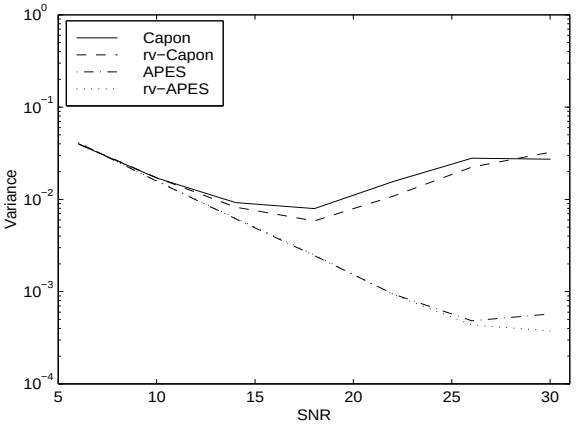

Figure 4: The presented estimators' variance as the SNR varies.

Capon estimator have a (slightly) lower variance than it's complex-valued counterpart, whereas the APES estimators have roughly the same variance.

It should be mentioned that the estimators performance varies somewhat with the frequency separation, but the case shown is typical. Our results are obtained from 1000 Monte Carlo trials.

5. REFERENCES

[1] P. Stoica, A. Jakobsson, and J. Li, "Matched-filter bank interpretation of some spectral estimators", *To appear in Signal Processing*, **66**(1).

[2] J. Li and P. Stoica, "Adaptive Filtering Approach to Spectral Estimation and SAR Imaging", *IEEE Trans. on Signal Processing*, **44**(6):1469–1484, June 1996.

[3] J. Capon, "High Resolution Frequency Wave Number Spectrum Analysis", *Proc. IEEE*, **57**:1408–1418, 1969.

[4] R. Lacoss, "Data adaptive spectral analysis methods", *Geophysics*, **36**:134–148, 1971.

[5] M.A. Lagunas, M.E. Santamaria, A. Gasull, and A. Moreno, "Maximum likelihood filters in spectral estimation problems", *Signal Processing*, **10**(1):19–34, 1986.

[6] P. Stoica and R. Moses, *Introduction to Spectral Analysis*, Prentice Hall, Upper Saddle River, NJ, 1997.